Liquid Crystals
Publication details, including instructions for authors and subscription information:
http://www.informaworld.com/smpp/title~content=t713926090

Ferroelectric liquid crystals induced by atropisomeric biphenyl dopants: the effect of chiral perturbations on achiral dopants

C. Scott Hartley[a]; Robert P. Lemieux Corresponding author[a]
[a] Department of Chemistry, Queen's University, Kingston, Ontario, Canada K7L 3N6

Online publication date: 12 May 2010

To cite this Article Hartley, C. Scott and Lemieux Corresponding author, Robert P.(2004) 'Ferroelectric liquid crystals induced by atropisomeric biphenyl dopants: the effect of chiral perturbations on achiral dopants', Liquid Crystals, 31: 8, 1101 — 1108
To link to this Article: DOI: 10.1080/02678290410001715999
URL: http://dx.doi.org/10.1080/02678290410001715999

LIQUID CRYSTALS, VOL. 31, NO. 8, AUGUST 2004, 1101–1108

Ferroelectric liquid crystals induced by atropisomeric biphenyl dopants: the effect of chiral perturbations on achiral dopants

C. SCOTT HARTLEY and ROBERT P. LEMIEUX*

Department of Chemistry, Queen's University, Kingston, Ontario, Canada K7L 3N6

(*Received 20 January 2004; accepted 31 March 2004*)

The addition of the achiral biphenyl dopant 2,2′,6,6′-tetramethyl-4,4′-bis(4-*n*-nonyloxybenzoyloxy)biphenyl (**3**) or its dithionoester or dithioester analogue (**4**, **5**) to a 4 mol% mixture of the atropisomeric biphenyl dopant (*R*)-2,2′,6,6′-tetramethyl-3,3′-dinitro-4,4′-bis(4-*n*-nonyloxybenzoyloxy)biphenyl, (*R*)-**1**, in the phenylpyrimidine SmC host **PhP1** produces a significant amplification of the spontaneous polarization induced by (*R*)-**1**. This amplification may be due to a chiral perturbation by (*R*)-**1** which causes a shift in the equilibrium between enantiomeric conformations of the achiral dopant. The degree of polarization amplification afforded by the achiral dopant, as expressed by the polarization amplification factor *PAF*, varies with the nature of the linking group. This may be ascribed to different rotational distributions of the core transverse dipole moments relative to the polar axis of the SmC* phase and/or to differences in lateral bulk of the polar linking groups. The latter may affect the degree of chiral molecular recognition achieved by **3**–**5** in the binding site of the SmC* phase.

1. Introduction

Over the past two decades, much research activity in liquid crystal science has focused on the development of chiral smectic liquid crystals, including ferroelectric SmC*, antiferroelectric SmC_a^* and electroclinic SmA* phases, due to their potential as electro-optical materials for the next generation of display applications [1]. Already, colour viewfinders based on high resolution reflective ferroelectric liquid crystal (FLC) microdisplay technology can be found in commercial products such as digital cameras and camcorders [2, 3]. In a surface-stabilized planar alignment, SmC* liquid crystals exhibit a spontaneous polarization $\mathbf{P}_S$ that coincides with the polar C_2 symmetry axis of the SmC* phase (polar axis). The spontaneous polarization is a macroscopic manifestation of molecular chirality which originates from a conformational bias of transverse molecular dipoles to orient in one direction along the polar axis [4, 5]. In most cases, this polar conformational bias is intrinsic to the chiral molecules and arises from steric coupling of polar functional groups to one or more stereogenic centre(s), which form a stereo-polar structural unit. In this study, we show that a polar conformational bias may also be induced in achiral molecules by chiral perturbations exerted by an atropisomeric biphenyl dopant.

An important aspect of FLC materials research is the understanding of the relationship between the molecular structure of the chiral constituent(s) of a SmC* liquid crystal and the magnitude of $\mathbf{P}_S$. In commercial FLC mixtures, the spontaneous polarization is induced by mixing small amounts of a chiral dopant with high polarization power into an achiral SmC mixture with low viscosity and wide temperature range. The polarization power δ_p is a measure of the propensity of a chiral dopant to induce a polarization according to equation (1), where x_d is the dopant mole fraction and $\mathbf{P}_o$ is the reduced polarization normalized for variations in tilt angle θ according to equation (2) [6, 7].

$$\delta_p = \left(\frac{d\mathbf{P}_o(x_d)}{dx_d}\right)_{x_d \to 0} \quad (1)$$

$$\mathbf{P}_o = \mathbf{P}_s/\sin\,\theta. \quad (2)$$

The vast majority of chiral dopants found in FLC formulations have stereo-polar units located in one of the side chains and generally exhibit polarization powers that are invariant with respect to the SmC host structure (type I dopants) [8]. This behaviour is consistent with the Boulder model for the molecular origins of $\mathbf{P}_S$ [4, 9, 10]. According to this model, the SmC phase is considered to be a supramolecular host,

*Author for correspondence;
e-mail: lemieux@chem.queensu.ca

Liquid Crystals ISSN 0267-8292 print/ISSN 1366-5855 online © 2004 Taylor & Francis Ltd
http://www.tandf.co.uk/journals
DOI: 10.1080/02678290410001715999

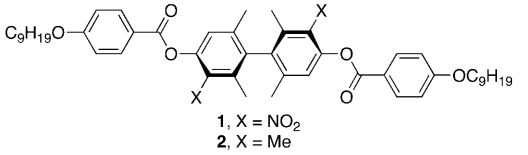

1, X = NO_2
2, X = Me

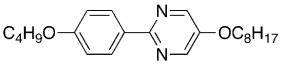

PhP1: Cr 58 SmC 85 SmA 95 N 98 I

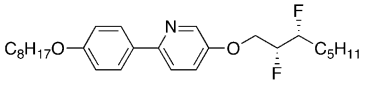

MDW950

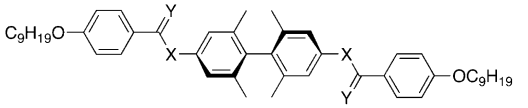

3, X,Y = O
4, X = O, Y = S
5, X = S, Y = O

and the conformational and orientational ordering of a chiral dopant in the SmC host is modelled by a mean field potential which qualitatively behaves like a binding site analogous to that described in host–guest chemistry. Within the confines of this binding site, which is shaped like a bent cylinder with C_{2h} symmetry, the orientational distribution of a chiral dopant along its long molecular axis acquires a polar character. Such polar ordering, combined with the conformational asymmetry of the stereo-polar unit, results in an orientational bias of the dopant's transverse dipole moment $\mu_\perp$ along the polar C_2 axis. The shape of the binding site is assumed to be invariant with respect to the SmC host structure, and the Boulder model assumes that a chiral dopant plays the role of a *passive* guest which adopts a conformation that best fits the achiral binding site.

Unlike conventional dopants with chiral side-chains, dopants with stereo-polar units located in the rigid aromatic core tend to exhibit polarization powers that vary significantly with the structure of the SmC host (type II dopants) [8]. This host effect is thought to originate from rigid core–core interactions between chiral dopant and surrounding host molecules and may be viewed as a manifestation of host–guest molecular recognition that cannot be achieved with type I dopants due to the higher degree of conformational disorder among side chains in the diffuse layer structure of the SmC phase [11]. In other words, the shape invariance assumption of the Boulder model for the SmC binding site appears to break down in the case of type II dopants. We have shown that the polarization power of chiral dopants with atropisomeric biphenyl cores, e.g. (*R*)-**1**, depends very strongly on the core structure of the SmC host [12]. Some of these dopants exhibit polarization powers as high as 1738 $nC\,cm^{-2}$ in hosts with a 2-phenylpyrimidine core (e.g. **PhP1**), but less than 35 $nC\,cm^{-2}$ in hosts with a phenyl benzoate core. Experimental evidence suggests that, unlike conventional type I dopants, these chiral dopants behave as *active* guests causing a strong chiral perturbation of the SmC host [13–15]. Such chiral perturbation is most likely achieved by inducing homochiral core conformations in surrounding host molecules via core–core interactions (i.e. chirality transfer), as shown in figure 1. This empirical model is consistent with the complementarity of dopant/host core structures in **PhP1**, or lack thereof in phenyl benzoate SmC hosts, and was originally invoked by Gottarelli and coworkers to account for the unusually high helical twisting powers of atropisomeric binaphthyl dopants in nematic hosts such as 5CB [16, 17]. We proposed that one possible outcome of chiral perturbations exerted by dopants such as (*R*)-**1** is a chiral distortion of the binding site topography, as shown in figure 2, which

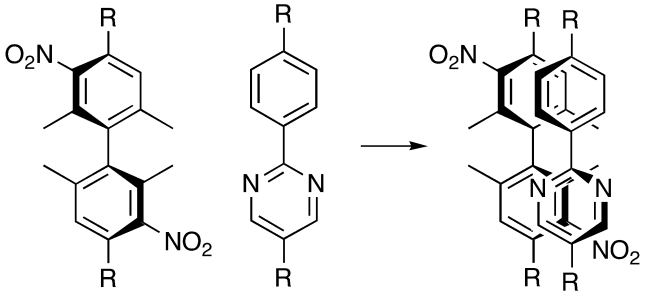

Figure 1. Model for chirality transfer between dopant **1** and **PhP1** via core–core conformational interactions.

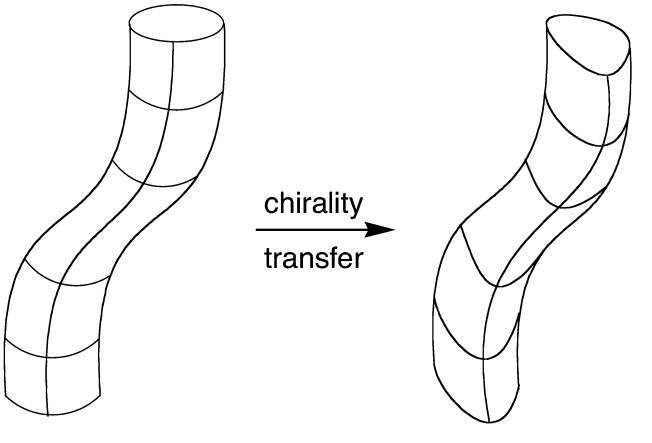

Figure 2. Chiral distortion of the SmC binding site according to the CTF model. The polar axis is normal to the plane of the page.

results in the amplification of δ_p as a chirality transfer feedback (CTF) [12]. The CTF effect may take the form of a shift in orientational distribution of the dopant $\mu_\perp$ with respect to the polar axis and/or a shift in the conformational distribution of the stereo-polar unit favoring one orientation of $\mu_\perp$ along the polar axis.

To test the CTF model, we measured the effect of perturbations exerted by each enantiomer of dopant **1** on the polarization power of the chiral probe molecule **MDW950**, which mimics the structure of **PhP1** [14]. The results showed that the polarization power of the probe decreases in the presence of (*R*)-**1** and increases in the presence of (*S*)-**1**, which is consistent with a *chiral* perturbation influencing the conformational distribution of the chiral probe. Further evidence supporting the CTF model was provided by another experiment in which the two enantiomers of dopant **2** were used as probes in the presence of (*S*)-**1**. The results showed that the perturbation exerted by (*S*)-**1** amplified the polarization powers of (+)-**2** and (−)-**2** by factors of 5.5 and 2.8, respectively. More significantly, the perturbation caused an inversion of the sign of $\mathbf{P}_S$ induced by (−)-**2**, which is consistent with the chiral nature of the perturbation exerted by (*S*)-**1** and shows that such perturbation can amplify the polarization power of another atropisomeric dopant. More recently, we showed that the polarization power of (*R*)-**1** in **PhP1** can be amplified upon addition of an isostructural smectic co-host with a non-planar 5-phenylpyrimidine core [15].† Similar observations of chiral amplification were also reported upon addition of achiral bent core dopants in chiral nematic and SmC* liquid crystals [19, 20]. These results may be ascribed to a shift in the conformational equilibrium of the dynamically racemic additives towards one enantiomeric conformation which, in turn, may amplify chiral bulk properties and/or enhance the propagation of chiral perturbations.

The rational design of achiral additives capable of amplifying the polarization of a FLC based on molecular recognition principles could prove useful in the formulation of commercial SmC* mixtures because of the lower cost of achiral materials. To investigate the scope of polarization amplification using achiral additives, and the contribution of ester linking groups in the induction of polarization by atropisomeric biphenyl dopants, we synthesized the achiral dopants **3**–**5** and measured their effect on the polarization induced by (*R*)-**1** in **PhP1**.

†*Ab initio* calculations suggest that the 2-phenylpyrimidine core of **PhP1** adopts a planar conformation in the ground state.

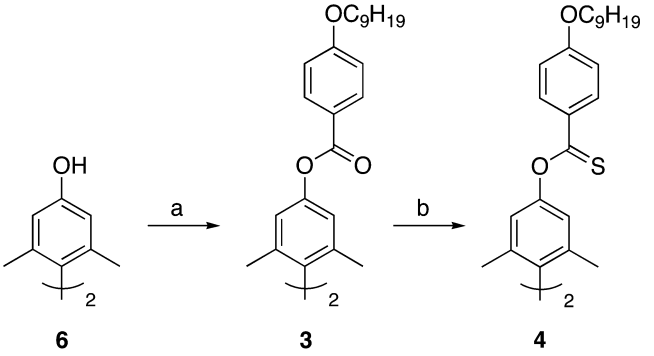

Scheme 1. *Reagents and conditions*: (*a*) 4-nonyloxybenzoic acid, DCC, DMAP, CH_2Cl_2, 25°C; (*b*) Lawesson's reagent, *m*-xylene, reflux.

2. Results

2.1. *Synthesis*

The dopants **3**–**5** were derived from the known dihydroxybiphenyl **6** [13], as shown in schemes 1 and 2. Dopant **3** was obtained by esterification of **6** with 4-nonyloxybenzoic acid and DCC/DMAP in 90% yield, and was converted to the corresponding dithionoester **4** by treatment with Lawesson's reagent in 32% yield [21]. The synthesis of dopant **5** began with conversion of **6** to the dithionocarbamate **7** in 63% yield, followed by rearrangement to the corresponding dithiocarbamate **8** in 88% yield upon heating under reflux in diphenyl ether. Hydrolysis of **8** and subsequent esterification with 4-nonyloxybenzoic acid and DCC/DMAP gave dopant **5** in 35% yield.

2.2. *Polarization measurements*

The reduced polarization $\mathbf{P}_o$ induced by dopant (*R*)-**1** (4 mol%) in the presence of each of the achiral dopants **3**–**5** was measured as a function of the mole fraction of achiral dopant x_{ad} over the range $0 < x_{ad} \leqslant 0.05$ at a reduced temperature $T - T_C = -5$ K. To minimize

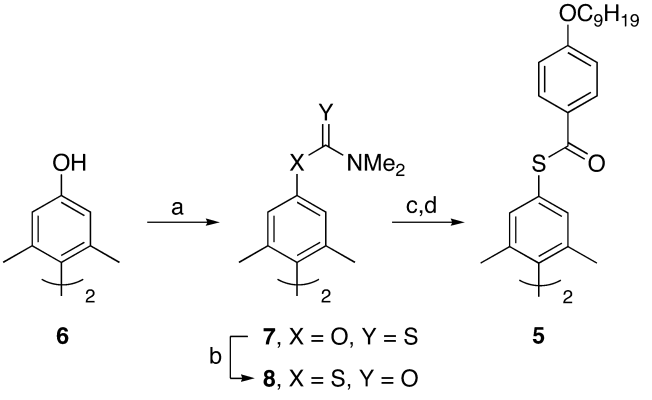

Scheme 2. *Reagents and conditions*: (*a*) $Me_2NC(S)Cl$, NaH, DMF, 25°C; (*b*) Ph_2O, reflux; (*c*) NaOH, EtOH, reflux; (*d*) 4-nonyloxybenzoic acid, DCC, DMAP, CH_2Cl_2, 25°C.

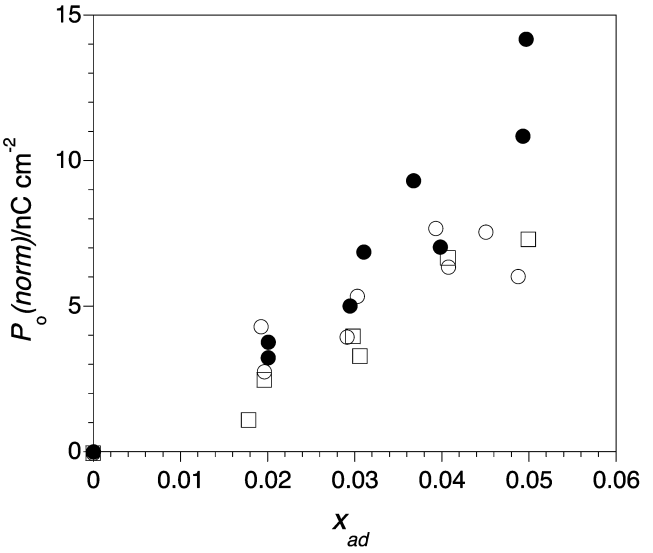

Figure 3. Normalized reduced polarization $\mathbf{P}_o(norm)$ vs mole fraction of achiral dopant x_{ad}: **3** (filled circles), **4** (open circles), **5** (open squares).

weighing errors, dopants **3**–**5** were mixed in a 4.1 mol% stock solution of (*R*)-**1** in **PhP1** ($x_1 = 0.041$), which results in a slight decrease in x_1 from 0.041 to 0.039 with increasing mole fraction of achiral dopant. The reduced polarization values obtained experimentally $\mathbf{P}_o(exp)$ are normalized by subtracting the calculated contribution from the atropisomeric dopant $\mathbf{P}_o(\mathbf{1})$ in the absence of achiral dopant, taking into account the variation in x_1 caused by dilution, according to equation (3). The resulting plots of $\mathbf{P}_o(norm)$ vs x_{ad} show that the addition of any of the three achiral dopants **3**–**5** results in amplification of the polarization induced by the atropisomeric dopant (*R*)-**1** (figure 3). The degree of polarization amplification afforded by each achiral dopant is expressed by the *polarization amplification factor (PAF)* according to equation (4), which is similar in form to the polarization power of a chiral dopant [22]. *PAF* values for dopants **3**–**5** are given in the table along with transverse dipole moments $\mu_\perp$ of the functionalized biphenyl core calculated at the AM1 level (*vide infra*). Statistical analysis using the Student *t*-test reveals that the *PAF* for dopant **3** is significantly larger than the other two at the 95% confidence level. However, *PAF* values for **4** and **5** cannot be distinguished statistically at a confidence level of $\geqslant 60\%$.

Table 1. Polarization amplification factors *PAF* for dopants **3**, **4** and **5** in a 4 mol% mixture of (*R*)-**1** in **PhP1** and transverse dipole moments $\mu_\perp$ of the functionalized biphenyl cores in their lowest energy conformation calculated at the AM1 level.

Dopant	*PAF*/nC cm^{-2}[a]	$\mu_\perp$/*D*
3	257 ± 34	1.94
4	159 ± 20[b]	2.62
5	146 ± 23[b]	1.82

[a]Uncertainty is ±standard error of the least-squares fit.
[b]These two values cannot be distinguished statistically at a confidence level of $\geqslant 60\%$.

$$\mathbf{P}_o(norm) = |\mathbf{P}_o(exp)| - |\mathbf{P}_o(\mathbf{1})| \quad (3)$$

$$PAF = \left(\frac{d\mathbf{P}_o(norm)}{dx_{ad}}\right)_{x_{ad}\to 0} . \quad (4)$$

3. Discussion

The *PAF* is conceptually similar to the polarization power of a chiral dopant as it measures the contribution of a 'chirally distorted' dopant to the polarization of the SmC* mixture. Within experimental error, the *PAF* value of diester **3** is equal in magnitude to the polarization power of one enantiomer of **2** measured in the presence of (*S*)-**1** at 4 mol% (256 ± 36 nC cm^{-2}), which suggests that the chiral perturbation exerted by **1** influences the conformational distributions of the two diesters in a similar way. According to a conformational analysis of the ester group at the AM1 level (figure 4), the C(O)–O single bond in **3** forms a dihedral angle of *c.* 50° with the plane of the phenyl ring. Assuming that all dopants adopt a zigzag conformation in the SmC* phase that conforms to the binding site of the Boulder model (figure 2), the conformational

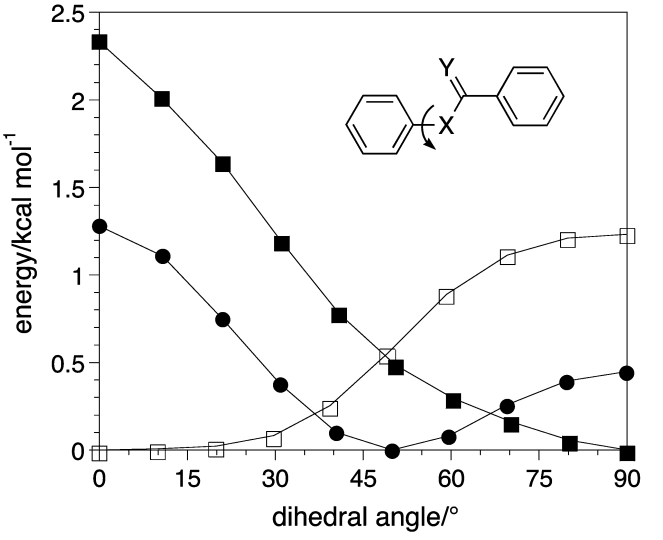

Figure 4. Relative energy as a function of the dihedral angle formed by the C(*Y*)–*X* bond and the plane of the phenyl ring in model compounds (inset) calculated at the AM1 level: *X*, *Y* = O (circles); *X* = O, *Y* = S (filled squares); *X* = S, *Y* = O (open squares).

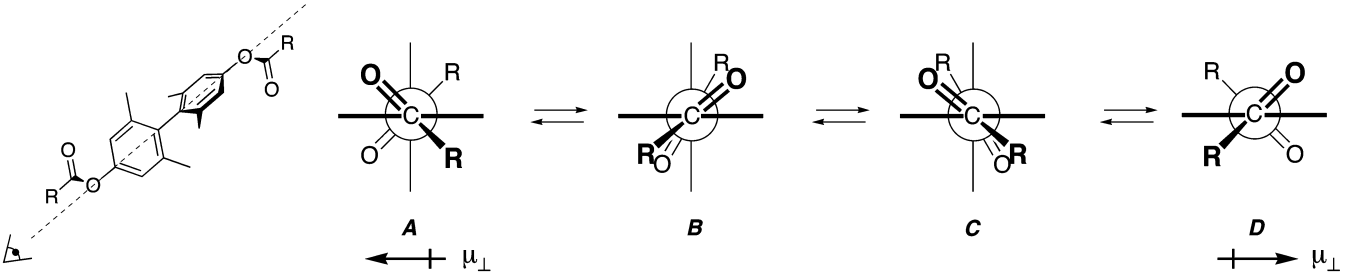

Figure 5. Approximate conformational distribution of the ester linking groups for dopant **3** in a zigzag conformation shown as Newman projections along the central C–C bond of the biphenyl core. The polar axis of the SmC* phase is oriented horizontally in the plane of the page relative to the Newman projections.

distribution of the two ester groups may therefore be approximated by figure 5, in which the angle formed by the two C=O bonds along the long axis of the core–diester unit is either 90° or 180°. One must note that this conformational distribution is an oversimplification of a complex conformational/orientational hypersurface, but it does provide a useful basis to understand the effect of chiral perturbations on polar order. In the case of dopant **3**, the chiral conformations *A* and *D* are enantiomeric and should be of equal energy in an achiral environment. In a chiral environment, one enantiomeric conformation should be energetically favoured and thus contribute to the polarization of the SmC* phase (the chiral conformations *B* and *C* have negligible $\mu_\perp$ and their contribution to $\mathbf{P}_S$ may be ignored in this analysis). At the same level of approximation, the conformational distribution of dopant **2** is restricted to either *A* or *D*, depending on the absolute configuration of the atropisomeric core, due to steric repulsion between the ester carbonyl and *ortho*-methyl groups.

According to the CTF model, a strong chiral perturbation exerted by one enantiomer of **1** should cause a chiral distortion of the binding site that 'fits' one enantiomeric conformation of the dopant better than the other. In the case of dopant **2**, this difference in fit coupled with the intrinsic preference for conformation *A* or *D* results in a difference in polarization power for the two enantiomers (+)-**2** and (−)-**2** (256 vs 130 nC cm^{-2}, respectively). On the other hand, dopant **3** has no intrinsic preference for *A* or *D* and can therefore respond to the chiral perturbation by adopting the enantiomeric conformation that best fits the chirally distorted binding site. The agreement between the *PAF* value for **3** and one of the two δ_p values obtained for **2** under the same conditions is consistent with this explanation.

Conformational analyses of the thionoester and thioester linking groups suggest that the conformational distributions of dopants **4** and **5** in the binding site of the SmC* phase should be similar to that of **3**, but include only enantiomeric conformations similar to *A* and *D* (figure 6). As shown in figure 4, the calculations predict that the C(S)–O single bond in **4** forms a dihedral angle of 90° with the plane of the phenyl ring, and that the C(O)–S single bond in **5** is co-planar with the phenyl ring. In each case, the angle formed by the two C=X double bonds along the long axis of the orthogonal biphenyl core should be approximately 90°. Despite the predicted similarity in conformational distribution, the *PAF* values of **3**–**5** do not scale with the transverse dipole moments $\mu_\perp$ of the functionalized biphenyl cores calculated at the AM1 level. This may be ascribed to different rotational distributions of the core

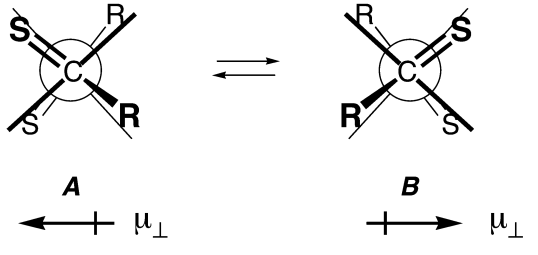

Figure 6. Approximate conformational distribution of the thionoester linking groups for dopant **4** shown as Newman projections along the central C–C bond of the biphenyl core. The polar axis of the SmC* phase is oriented horizontally in the plane of the page.

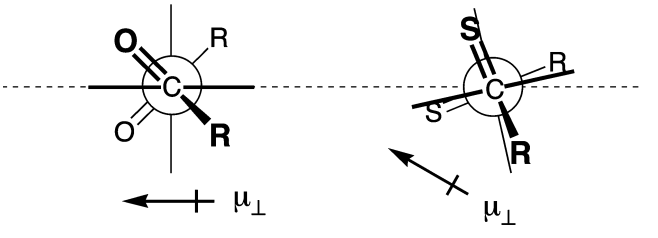

Figure 7. Different rotational distributions of the transverse dipole moments $\mu_\perp$ for dopants **3** (left) and **4** (right) in their lowest energy conformations relative to the polar axis of the SmC* phase (dotted line).

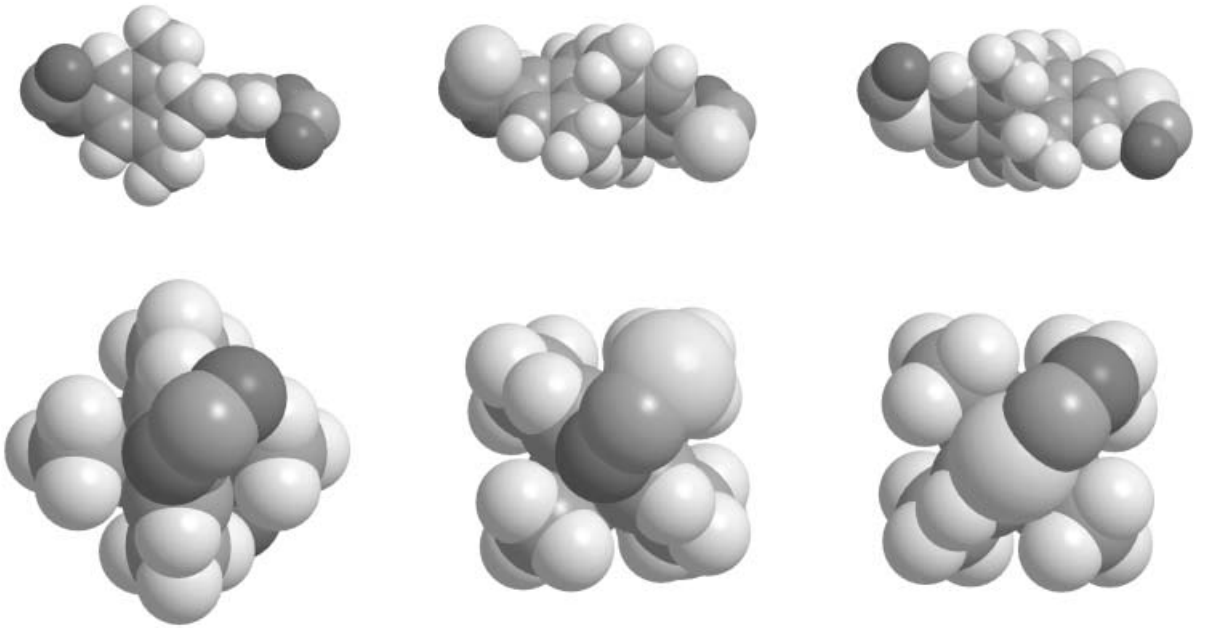

Figure 8. Space-filling models (AM1) of the functionalized biphenyl cores of dopants **3**, **4** and **5** (from left to right) viewed along the polar axis (top) and along the central C–C bond of the biphenyl core (bottom). The 4-alkoxyphenyl fragments are hidden for clarity.

transverse dipole moments relative to the polar axis of the SmC* phase, as shown in figure 7. Another possible explanation for the lack of correlation between *PAF* and $\mu_{\perp}$ is rooted in differences in lateral bulk of the polar linking groups. For example, the thionoester linking group in **4** is significantly more bulky than the diester linking group in **3** (figure 8), which may affect how the functionalized biphenyl core senses the chiral perturbation exerted by **1**. In the case of a bulkier linking group, the *PAF* could be reduced by an increase in free volume between dopant and host molecules due to steric repulsion, which would effectively loosen the binding site and reduce the effect of any chiral perturbation on the conformational distribution of the dopant.

4. Conclusions

We have shown that the addition of achiral biphenyl dopants **3**–**5** to a 4 mol% mixture of the atropisomeric biphenyl dopant (*R*)-**1** in the phenylpyrimidine SmC host **PhP1** produces a significant amplification of the spontaneous polarization induced by (*R*)-**1**. This amplification may be ascribed to a chiral perturbation by (*R*)-**1** that causes a shift in the equilibrium between enantiomeric conformations of the achiral dopant with transverse dipole moments oriented along the polar axis of the SmC* phase. The degree of polarization amplification, as expressed by the polarization amplification factor *PAF*, varies with the nature of the linking group, which may be ascribed to different rotational distributions of the core transverse dipole moments relative to the polar axis of the SmC* phase and/or to differences in lateral bulk of the polar linking groups. The latter may affect the degree of chiral molecular recognition achieved by **3**–**5** in the binding site. Indeed, these results suggest that the ester linking groups coupled to the atropisomeric dinitrobiphenyl core make a significant contribution to the chiral perturbation exerted by (*R*)-**1** in **PhP1**.

5. Experimental

5.1. *General*

^{1}H and ^{13}C spectra were recorded on Bruker Avance 400 spectrometers in deuterated chloroform. Chemical shifts are reported in δ (ppm) relative to tetramethylsilane. Low resolution EI mass spectra were recorded on a Fisons VG Quattro triple quadrupole mass spectrometer; peaks are reported as *m*/*z* (% intensity relative to the base peak). High resolution EI mass spectra were performed by the University of Toronto mass spectrometry facility. Elemental analysis was performed by Canadian Microanalytical Service Ltd. (Delta, British Columbia). Melting points were measured on a Fisher–Johns melting point apparatus and are uncorrected. Conformational analyses and transverse dipole moment calculations were performed at the AM1 level using MOPAC 97 as implemented on Chem3D Pro version 4.0.

5.2. *Synthesis*

All reagents, chemicals and liquid crystal hosts were obtained from commercial sources and used without further purification unless otherwise noted. Tetrahydrofuran (THF) was distilled from sodium/benzophenone under argon. (*R*)-2,2′,6,6′-Tetramethyl-3,3′-dinitro-4,4′-bis(4-*n*-nonyloxybenzoyloxy)biphenyl, (*R*)-**1**, and 4,4′-dihydroxy-2,2′,6,6′-tetramethylbiphenyl, **6**, were synthesized according to literature procedures and shown to have the expected physical and spectral properties [13].

5.2.1. *2,2′,6,6′-Tetramethyl-4,4′-bis(4-n-nonyloxybenzoyloxy)biphenyl (**3**)*

To a stirred solution of **6** (166 mg, 0.62 mmol), *p*-nonyloxybenzoic acid (500 mg, 1.9 mmol) and DMAP (230 mg, 1.88 mmol) in CH_2Cl_2 (20 ml) was added solid DCC (390 mg, 1.9 mmol). The mixture was stirred at room temperature under N_2 overnight, then filtered, diluted with EtOAc and washed with 2% aq. HCl (2 ×), water and brine. The organic layer was dried ($MgSO_4$), concentrated, and the residue purified by flash chromatography on silica gel (9/1 hexanes/EtOAc). Recrystallization from hexanes gave 407 mg (90%) of **3** as a white solid. Before doping into liquid crystal mixtures, the compound was again recrystallized from hexanes after filtration through a 0.45 µm PTFE filter: m.p. 114–115°C. ^{1}H NMR ($CDCl_3$, 400 MHz) δ 0.89 (t, J = 6.4 Hz, 6H), 1.30 (m, 20H), 1.48 (m, 4H), 1.83 (m, 4H), 1.95 (s, 12H), 4.05 (t, J = 6.8 Hz, 4H), 6.98 (d, J = 8.8 Hz, 4H), 7.01 (s, 4H), 8.15 (d, J = 8.8 Hz, 4H). ^{13}C NMR ($CDCl_3$, 100 MHz) δ 14.3, 20.1, 22.8, 26.2, 29.3, 29.4, 29.5, 29.7, 32.0, 68.5, 114.4, 120.7, 122.0, 132.4, 136.8, 137.5, 150.0, 163.6, 165.2. Anal: calcd for $C_{48}H_{62}O_6$ C 78.44, H, 8.50; found C 78.44, H 8.43%.

5.2.2. *2,2′,6,6′-Tetramethyl-4,4′-bis(4-n-nonyloxybenzothioyloxy)biphenyl (**4**)*

A stirred mixture of **3** (128 mg, 0.18 mmol) and Lawesson's reagent (350 mg, 0.87 mmol) in *m*-xylene (2 ml) was heated under reflux under N_2 overnight. The mixture was then cooled and eluted on a silica gel column (9/1 hexanes/EtOAc) to give 43 mg (32%) of **4** as a yellow solid. Before doping into liquid crystal mixtures, the compound was recrystallized from hexanes after filtration through a 0.45 µm PTFE filter to give yellow needles: m.p. 121–122°C. ^{1}H NMR ($CDCl_3$, 400 MHz) δ 0.89 (t, J = 6.6 Hz, 6H), 1.2–1.4 (m, 20H), 1.48 (m, 4H), 1.83 (4H), 1.99 (s, 12H), 4.06 (t, J = 6.4 Hz, 4H), 6.92 (m, 8H), 8.36 (d, J = 8.9 Hz, 4H). ^{13}C NMR ($CDCl_3$, 100 MHz) δ 14.3, 20.1, 22.8, 26.1, 29.3, 29.4, 29.5, 29.7, 32.0, 68.6, 114.1, 121.2, 131.3, 131.8, 137.2, 137.5, 153.9, 163.9, 210.1. Anal: calcd for $C_{48}H_{62}O_4S_2$ C 75.15, H 8.15, S 8.36; found C 74.98, H 8.15, S 8.48%.

5.2.3. *2,2′,6,6′-Tetramethyl-4,4′-bis(O-dimethylthiocarbamoyloxy)biphenyl (**7**)*

To a stirred solution of **6** (128 mg, 0.53 mmol) in dry DMF (2 ml) was added NaH as a 60% dispersion in mineral oil (98 mg, 2.4 mmol). The mixture was stirred for 25 min at room temperature and a solution of dimethylthiocarbamoyl chloride (277 mg, 2.24 mmol) in dry DMF (1 ml) was added dropwise. This mixture was stirred overnight under N_2, then poured into water (50 ml) and extracted with Et_2O (3 ×). The combined extracts were washed with water and brine, dried ($MgSO_4$) and concentrated. The residue was purified by flash chromatography on silica gel (4/1 hexanes/EtOAc) to give 138 mg (63%) of **7** as a white solid: m.p. 214–219°C. ^{1}H NMR ($CDCl_3$, 400 MHz) δ 1.93 (s, 12H), 3.55 (s, 6H), 3.48 (s, 6H), 6.85 (s, 4H). ^{13}C NMR ($CDCl_3$, 100 MHz) δ 20.1, 38.8, 43.4, 121.6, 136.9, 137.2, 153.0, 188.0. MS (EI) *m/z* 416 (M^+, 1), 88 (93), 72 (100). HRMS (EI): calcd for $C_{22}H_{28}N_2O_2S_2$ 416.1592; found 416.1603.

5.2.4. *2,2′,6,6′-Tetramethyl-4,4′-bis(S-dimethylcarbamoylsulfanyl)biphenyl (**8**)*

A stirred solution of **7** (117 mg, 0.28 mmol) in diphenyl ether (1 ml) was heated under reflux for 3 h. The solution was then cooled and eluted on a silica gel column, first with hexanes to remove the diphenyl ether, then with EtOAc to give 102 mg (88%) of **8** as a white solid: m.p. 283–285°C. ^{1}H NMR ($CDCl_3$, 400 MHz) δ 1.90 (s, 12H), 3.05 (br s, 6H), 3.11 (br s, 6H), 7.28 (s, 4H). ^{13}C NMR ($CDCl_3$, 100 MHz) δ 19.9, 37.1, 126.8, 134.9, 136.5, 140.6, 167.6; MS (EI) *m/z* 416 (M^+, 4), 72 (100). HRMS (EI): calcd for $C_{22}H_{28}N_2O_2S_2$ 416.1592; found 416.1589.

5.2.5. *2,2′,6,6′-Tetramethyl-4,4′-bis(4-n-nonyloxybenzoylsulfanyl)biphenyl (**5**)*

To a stirred mixture of **8** (79 mg, 0.19 mmol) in abs. EtOH (6 ml) was added a solution of NaOH (0.10 g, 2.5 mmol) in water (1 ml). The mixture was heated under reflux for 2 h, then cooled, poured into water (50 ml) and extracted with Et_2O. The organic layer was washed with water and brine, dried (Na_2SO_4) and concentrated. The resulting crude oil was dissolved in CH_2Cl_2 (7 ml) and treated with *p*-nonyloxybenzoic acid (159 mg, 0.60 mmol), DMAP (78 mg, 0.64 mmol) and DCC (139 mg, 0.67 mmol), and stirred at room

temperature overnight under N_2. The mixture was then filtered, diluted with EtOAc, washed with 1% aq. HCl (2×) and brine (2×), dried (Na_2SO_4) and concentrated. The residue was purified by flash chromatography on silica gel (9/1 hexanes/EtOAc) and recrystallized from hexanes to give 52 mg (35%) of **5** as a white solid. Before doping into liquid crystal mixtures, the compound was recrystallized from hexanes after filtration through a 0.45 μm PTFE filter: m.p. 123–126°C. ^{1}H NMR ($CDCl_3$, 400 MHz) δ 0.89 (t, $J=6.8$ Hz, 6H), 1.2–1.4 (m, 20H), 1.47 (m, 4H), 1.82 (m, 4H), 1.97 (s, 12H), 4.04 (t, $J=6.6$ Hz, 4H), 6.96 (d, $J=9$ Hz, 4H), 7.31 (s, 4H), 8.02 (d, $J=8.9$ Hz, 4H). ^{13}C NMR ($CDCl_3$, 100 MHz) δ 14.3, 20.0, 22.8, 26.1, 29.2, 29.4, 29.5, 29.7, 32.0, 68.5, 114.5, 126.0, 129.4, 129.8, 134.3, 136.8, 140.7, 163.8, 189.3. Anal: calcd for $C_{48}H_{62}O_4S_2$ C 75.15, H 8.15, S 8.36; found C 75.14, H 8.07, S 8.18%.

5.3. *Ferroelectric polarization measurements*

Texture analyses and transition temperature measurements for the doped liquid crystal mixtures were performed using a Nikon Labophot-2 POL polarizing microscope fitted with a Linkam LTS 350 hot stage. Spontaneous polarizations ($\mathbf{P}_S$) were measured at 5 K below the SmA*–SmC* transition temperature ($T-T_C=-5$ K) by the triangular wave method (6 V μm^{-1}, 100 Hz) [23]. Polyimide-coated ITO glass cells (4 μm × 0.16 cm^2) supplied by E.H.C. Co. were used for all the measurements. Good alignment was obtained by slow cooling of the filled cells from the isotropic phase via the N* and SmA* phases. Tilt angles (θ) were measured at $T-T_C=-5$ K between crossed polarizers as half the rotation between the two extinction positions corresponding to opposite polarization directions. The sign of $\mathbf{P}_S$ along the polar axis was assigned from the relative configuration of the electric field and the switching position of the sample according to the established convention [4]. Reduced polarization ($\mathbf{P}_o$) values were then obtained as $\mathbf{P}_S/\sin\theta$.

We are grateful to the Natural Sciences and Engineering Research Council of Canada, the Canada Foundation for Innovation and the Ontario Challenge Fund for support of this work.

References

[1] (*a*) Lagerwall, S. T. 1999, *Ferroelectric and Antiferroelectric Liquid Crystals*; Weinheim: Wiley-VCH; (*b*) Clark, N. A., and Lagerwall, S. T., 1991, in *Ferroelectric Liquid Crystals: Principles, Properties and Applications*, edited by J. W. Goodby, R. Blinc, N. A. Clark, S. T. Lagerwall, M. A. Osipov, S. A. Pikin, T. Sakurai, K. Yoshino, and B. Zeks, Philadelphia: Gordon and Breach, pp. 409–452; (*c*) Dijon, J. 1990, in *Liquid Crystals: Applications and Uses*, Vol. 1; edited by B. Bahadur, Singapore World Scientific, Chap. 13.

[2] Lagerwall, S. T., 1998, in *Handbook of Liquid Crystals*, Vol. 2B, edited by D. Demus, J. W. Goodby, G. W. Gray, H. W. Spiess, and V. Vill, Weinheim: Wiley-VCH.

[3] Walba, D. M., 1995, *Science*, **270,** 250.

[4] Walba, D. M., 1991, in *Advances in the Synthesis and Reactivity of Solids*, Vol. 1, edited by T. E. Mallouck, Greenwich, CT: JAI Press, pp. 173–235.

[5] (*a*) Goodby, J. W., Chin, E., Leslie, T. M., Geary, J. M., and Patel, J. S., 1986, *J. Am. chem. Soc.*, **108**, 4729; (*b*) Goodby, J. W., and Chin, E., 1986, *J. Am. chem. Soc.*, **108**, 4736.

[6] Siemensmeyer, K., and Stegemeyer, H., 1988, *Chem. Phys. Lett.*, **148,** 409.

[7] Kuczynski, W., and Stegemeyer, H., 1980, *Chem. Phys. Lett.*, **70,** 123.

[8] Stegemeyer, H., Meister, R., Hoffmann, U., Sprick, A., and Becker, A., 1995, *J. mater. Chem.*, **5,** 2183.

[9] Glaser, M. A., 1999, in *Advances in the Computer Simulations of Liquid Crystals*, edited by C. Zannoni, P. Pasini, Dordrecht: Kluwer, pp. 263–331.

[10] Glaser, M. A., Ginzburg, V. V., Clark, N. A., Garcia, E., Walba, D. M., and Malzbender, R., 1995, *Mol. Phys. Rep.*, **10,** 26.

[11] Tschierske, C., 1998, *J. mater. Chem.*, **8,** 1485.

[12] Lemieux, R. P., 2001, *Acc. chem. Res.*, **34,** 845.

[13] Vizitiu, D., Lazar, C., Halden, B. J., and Lemieux, R. P., 1999, *J. Am. chem. Soc.*, **121,** 8229.

[14] (*a*) Hartley, C. S., Lazar, C., Wand, M. D., and Lemieux, R. P., 2002, *J. Am. chem. Soc.*, **124**, 13513; (*b*) Lazar, C., Wand, M. D., and Lemieux, R. P., 2000, *J. Am. chem. Soc.*, **122**, 12586.

[15] Hegmann, T., and Lemieux, R. P., 2002, *J. mater. Chem.*, **12,** 3368.

[16] Gottarelli, G., Hibert, M., Samori, B., Solladié, G., Spada, G. P., and Zimmermann, R., 1983, *J. Am. chem. Soc.*, **105,** 7318.

[17] Spada, G. P., and Proni, G., 1998, *Enantiomer*, **3,** 301.

[18] Barone, V., Commisso, L., Lelj, F., and Russo, N., 1985, *Tetrahedron*, **41,** 1915.

[19] Thisayukta, J., Niwano, H., Takezoe, H., and Watanabe, J., 2002, *J. Am. chem. Soc.*, **124,** 3354.

[20] Gorecka, E., Cepic, M., Mieczkowski, J., Nakata, M., Takezoe, H., and Zeks, B., 2003, *Phys. Rev. E*, **67,** 061704.

[21] Pedersen, B. S., Scheibye, S., Clausen, K. and Lawesson, S.-O., 1978, *Bull. Soc. Chim. Belg.*, **87,** 293.

[22] Hegmann, T., Meadows, M. R., Wand, M. D., and Lemieux, R. P., 2004, *J. mater. Chem.*, **14,** 185.

[23] Miyasato, K., Abe, S., Takezoe, H., Fukuda, A., and Kuze, E., 1983, *Jpn. J. appl. Phys.*, **22,** L661.